Journal of the Neurological Sciences 398 (2019) 107–116

Contents lists available at ScienceDirect

Journal of the Neurological Sciences

journal homepage: www.elsevier.com/locate/jns

Amyloid PET pattern with dementia and amyloid angiopathy in Taiwan familial AD with D678H APP mutation

Chu-Yun Huang[a,b], Ing-Tsung Hsiao[c,d,1], Kun-Ju Lin[c,d,1], Kuo-Lun Huang[a], Hon-Chung Fung[a], Chi-Hung Liu[a], Ting-Yu Chang[a], Yi-Ching Weng[a], Wen-Chun Hsu[a], Tzu-Chen Yen[c,d,**], Chin-Chang Huang[a,e,*]

[a] Department of Neurology, Chang Gung Memorial Hospital, Taoyuan, Taiwan
[b] College of Pharmacy, Taipei Medical University, Taipei, Taiwan
[c] Molecular Imaging Center and Nuclear Medicine, Chang Gung University and Memorial Hospital, Taoyuan, Taiwan
[d] Medical Imaging and Radiological Sciences, Chang Gung University, Taoyuan, Taiwan
[e] College of Medicine, Chang Gung University, Taoyuan, Taiwan

ARTICLE INFO

Keywords:
Alzheimer's disease
Amyloid angiopathy
MRI
Taiwan APP mutation
D678H mutation
Brain AV-45 PET

ABSTRACT

Introduction: The novel D678H amyloid precursor protein (APP) gene mutation has been called the "Taiwan mutation". The study aims to identify amyloid deposition patterns and clinical features associated with this mutation.

Methods: we analyzed the clinical manifestations, brain neuroimages and ^{18}F-AV-45 positron emission tomography (PET) findings in symptomatic patients and asymptomatic subjects with the autosomal-dominant Alzheimer's disease (AD). We compared the amyloid deposition pattern among 10 patients with genetically-positive familial cognitive decline (CD), 18 patients with sporadic CD, and 19 healthy controls.

Results: The clinical features were the early onset of memory impairment in all 10 patients and cerebral amyloid angiopathy in 3 patients. The characteristic results of brain ^{18}F-AV-45 PET included the highest standard uptake value ratio (SUVR) in the occipital and cerebellar cortical areas in the genetically-positive CD patients. In subgroup analysis, the familial AD patients had a decreased amyloid SUVR trend in most areas except for cerebellar cortex compared to those with familial mild cognitive impairment.

Conclusion: Our data indicate that the familial D678H gene mutation have resulted in a more potent amyloid burden than in the patients with sporadic AD patients. The high amyloid uptake in the occipital area is characteristic of the specific Taiwan APP gene.

1. Introduction

Alzheimer's disease (AD) is a genetically dichotomous disease presenting as two forms: early-onset familial patients characterized by Mendelian inheritance, and late-onset with an inconsistent mode of transmission [1–3]. Three causative mutations, amyloid precursor protein (APP), presenilin 1 (PS1) and presenilin 2 (PS2), have been implicated in the pathogenesis of AD with an onset before or during the sixth decade of life [4–7]. In the APP gene, > 50 different mutations have been reported to be responsible for < 10% of familial cases of AD. The most common APP mutation is the London mutation (V717I) [8], which replaces the amino acid valine with isoleucine at protein position 717, leading to an increase in amyloid β peptide which then forms amyloid plaques in the brain.

At least six other APP mutations have been reported to cause hereditary cerebral amyloid angiopathy, characterized by strokes and a

Abbreviations: ADAS-Cog, Alzheimer's disease assessment scale-cognitive subscale; AD, Alzheimer's disease; Aβ, amyloid-β; APP, amyloid precursor protein; APoE, apolipoprotein; CD, cognitive decline; FAD, familial Alzheimer's disease; FLAIR, fluid attenuation inversion recovery; gAD, genetic Alzheimer's disease; gCD, genetic cognitive decline; HC, healthy control; MCI, mild cognitive impairment; MMSE, Mini-Mental State Examination; PCR, polymerase chain reaction; PS1, presenilin 1; PS2, presenilin 2; sAD, sporadic Alzheimer's disease; sCD, sporadic cognitive decline; SUVR, standard uptake value ratio; VOI, volume of interest

* Corresponding author at: Department of Neurology, Chang Gung Memorial Hospital, Chang Gung University, College of Medicine, No.5, Fuxing St., Guishan Township, Taoyuan, Taiwan.
** Corresponding author at: Molecular Imaging Center and Nuclear Medicine, Chang Gung University and Memorial Hospital, Taoyuan, Taiwan.
E-mail addresses: yen1110@cgmh.org.tw (T.-C. Yen), cch0537@adm.cgmh.org.tw (C.-C. Huang).
[1] Co-first author: Ing-Tsung Hsiao, PhD; Kun-Ju Lin, MD.

https://doi.org/10.1016/j.jns.2018.12.039
Received 26 September 2018; Received in revised form 26 December 2018; Accepted 31 December 2018
Available online 03 January 2019
0022-510X/

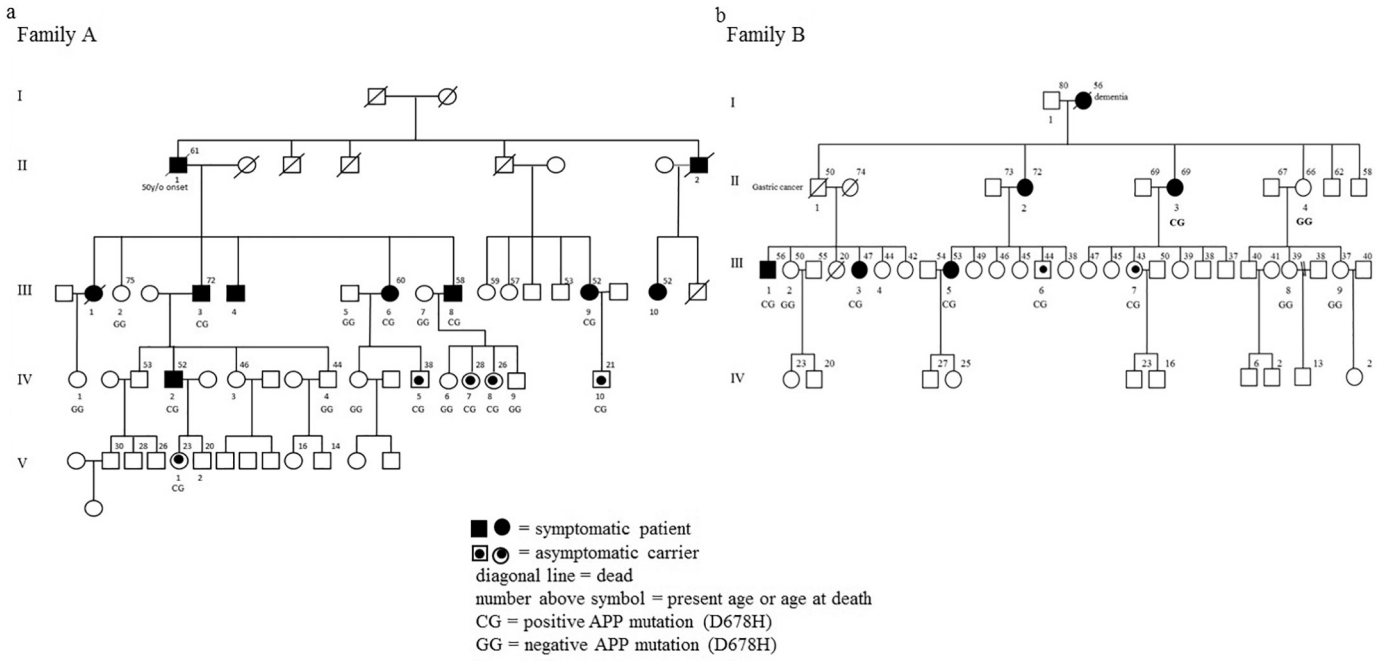

Fig. 1. The figure shows five and four generations of the two Taiwanese familial patients with autosomal dominant AD with the D678H APP mutation.

Table 1
Demographic data of the two Taiwanese familial patients with AD with the APP (D678H) mutation.

Subject No	Gender/Age (Y) (present age)	Onset age (Y)	Edu (Y)	Clinical features Initial → Follow up	Associated disease	MMSE Initial→Follow up	CDR Initial→ Follow up	APP (D678H) mutation	APoE gene
Symptomatic Family A									
A-III-3	M/72	48	2	MI → Delusion →Dementia → Stuporous	Subdural hematoma (postop)	8 → 0	2.0 → 4.0	CG	E3/E3
A-III-5	F/60	52	1	MI → Disorientation → Dementia	–	12 → 7	0.5 → 2 → 3.0	CG	E3/E3
A-III-6	M/58	47	9	MI → aMCI→ Delusion →Dementia	NPC (R/T)	21 → 16 → 1	0.5 → 2	CG	E3/E3
A-III-7	F/52	50	14	MI (aMCI)	–	26	0.5	CG	E3/E3
A-IV-2	M/52	50	9	MI (aMCI)	–	28	0.5	CG	E3/E3
Family B									
B-II-2	F/72	55	6	MI → Silly laughter →Delusion →Dementia	–	13 → 2	0.5 → 2.0	CG	E3/E3
B-II-3	F/69	53	6	MI → Delusion Hallucination →Dementia	–	14 → 2 → 0	1.0 → 2.0 → 3.0	CG	E3/E3
B-III-1	M/56	53	14	MI (aMCI)	–	19	0.5	CG	E3/E3
B-III-3	F/48	46	12	MI (aMCI)	–	28	0.5	CG	E3/E3
B-III-5	F/53	52	14	MI (aMCI)	–	26	0.5	CG	E2/E3
Asymptomatic Family A									
A-IV-5	M/38	–	18	–	–	30	0	CG	E3/E3
A-IV-7	F/28	–	15	–	–	30	0	CG	
A-IV-8	F/26	–	15	–	–	30	0	CG	
A-IV-10	M/21	–	15	–	–	30	0	CG	E3/E3
A-V-1	F/23	–	15	–	Head injury	28	0	CG	
Family B									
B-III-6	F/45	–	12	–	–	28	0	CG	E2/E3
B-III-7	F/43	–	16	–	–	28	0	CG	E3/E3

Y = year; Edu = education; MI = memory impairment; aMCI = amnestic mild cognitive impairment; MMSE = Mini Mental State Examination; CDR = Clinical Dementia Rating; M = male; F = female; NPC = nasopharyngeal cancer; R/T = radiation therapy.

decline in intellectual function in mid-adulthood. The Dutch mutation (E682Q) [9] is the most common, and others include the Italian type (E682K) [10], the Italian type (A713T) [11,12], the Flemish type (A692G) [13], the Iowa type (D694N) [14], and the Icelandic type (D673V) [15]. These mutations result in the production of amyloid β peptide which is prone to cluster and accumulate in the blood vessels of the brain. Amyloid then replace the muscle and elastic fibers resulting in a tendency to develop haemorrhagic strokes [16]. Recently, the novel APP mutation D678H was reported in Taiwan in two single cases [17,18]. The first case was a 59-year-old man with dementia and cerebral microvasculopathy [18]. Brain magnetic resonance imaging (MRI) showed leukoencephalopathy, cortical microhemorrhages, and

Table 2
Clinical progression of ten patients and seven asymptomatic members from the two Taiwanese familial patients with AD with the APP (D678H) mutation.

Subject No	Changes in cognitive function	Brain CT/MRI (Initial → follow up)	Brain AV-45 PET	Treatment
Symptomatic Family A				
A-III-3	Initial aMCI, disorientation, attention deficit, constructional apraxia, stuporous (post operation in 2005)	Mild CA (2001) → Diffuse CA, amyloid angiopathy, old cerebral haemorrhages, ventricular dilatation (2010)	↑F, T, P, Pre C, O	PI + R
A-III-5	disorientation, BPSD	Mild CA (2010) → Diffuse CA	↑F, T, P, Pre C, O	M + Q
A-III-6	aMCI, BPSD, disorientation, dementia	Mild CA (2003) → Diffuse CA	↑F, T, P, Pre C, O	G + M
A-III-7	aMCI	Normal, No HA (2010)	↑F, T, P, Pre C, O	D + M + PI
A-IV-2	aMCI	Normal, No HA (2010) →	↑ F, T, P, pre C, O	R1 + PI
Family B				
B-II-2	BPSD, disorientation, dementia	Diffuse CA + white matter lesion	↑ F, T, P, pre C, O	PI + Q
B-II-3	BPSD, disorientation, dementia	Diffuse CA + white matter lesion	↑ F, T, P, pre C, O	S + PI
B-III-1	aMCI, disorientation	Mild CA + white matter lesion	↑ F, T, P, pre C, O	D+ PI
B-III-3	aMCI	Mild CA	↑ F, T, P, pre C, O	D+ PI
B-III-5	aMCI	Mild CA, multiple microbleeds, amyloid angiopathy	↑ F, T, P, pre C, O	D
Asymptomatic Family A				
A-IV-5	Normal	Normal	Normal	
A-IV-7	Normal	NA	NA	
A-IV-8	Normal	NA	NA	
A-V-10	Normal	Normal	Normal	
A-V-1	Normal	NA	NA	
Family B				
B-III-6	Normal	Normal	Normal	
B-III-7	Normal	NA	NA	

aMCI = amnestic mild cognitive impairment; BPSD = behaviour and psychiatric symptoms of dementia; CA = cortical atrophy; HA = hippocampus atrophy; ↑ = increased uptake; F = frontal; P = parietal; T = temporal; pre C = precuneus; O = occipital; CT = computed tomography; MRI = magnetic resonance images; PET = positron emission tomography; NA: not available; PI = piracetam; R = risperidone; M = memantine; G = galantamine; RI = rivastigmine; Q = quantiapine; D = donepezil.

Table 3
Demographic data of the familial CD patients, sporadic CD patients and healthy controls.

	Familial CD patients (n = 10)	Sporadic CD patients (n = 18)	Healthy controls (n = 19)
Gender	4 M/6F	5 M/13F	10 M/9F
Ages (Y)(median)	48–72 (56)	55–79 (68.5)	48–76 (61.0)
Mean ± SD	59.2 ± 8.84	68.4 ± 7.93	61.16 ± 5.51
Education (Y)	1–14	0–16	0–21
Mean ± SD	8.7 ± 4.63	7.7 ± 5.3	12.4 ± 5.27
MMSE	0–28	8–21	26–30
CDR	0.5–4.0	0.5–1.0	0.0
APP gene	CG	GG	GG

CD: cognitive decline; M: male; F: female; Y: year; APP: amyloid precursor protein; CG: with positive D678H mutation; GG: without D678H mutation; *: p value > 0.05.

superficial cortical hemosiderosis. The mutation was also reported in a woman with progressive memory impairment at the age of 51, and slurred speech, restlessness, self-talking, inability to dress herself, and persecutory delusions [17]. Brain computed tomography (CT) revealed diffuse widening of cerebral fissures, cisterns, and sulci. This novel APP mutation D678H at chromosome 21: 27269917 G > C in exon 16 is a point missense mutation, and it has been called the Taiwan mutation [18]. Interestingly, the clinical features among these two cases of familial AD were different, although they were not clearly described.

[^{11}C]PIB positron emission tomography (PET) has been used to compare the amyloid plaque distribution among patients with AD [19,20]. Brain ^{18}F-florbetapir (AV-45/Amyvid) is recognized to be an effective amyloid beta (Aβ)-specific radiotracer in PET, and the results have been correlated with the extent of Aβ deposition found in the brain at autopsy in AD patients [21]. In our previous study, we compared the cerebral cortical amyloid load in healthy controls (HCs) and patients with AD, and found that the ^{18}F-AV-45 standard uptake value ratios (SUVRs) were higher in the frontal, anterior cingulate, parietal, temporal and precuneus areas [22]. In particular, the precuneus area was the most common area in the early stage of AD.

In this study, we analyzed the various clinical and genetic characteristics and amyloid deposition patterns using brain AV-45 PET in two large Taiwanese families with AD and the D678H APP mutation. We also compared the amyloid PET patterns among these patients with the Taiwan mutation, patients with sporadic AD, and HCs to elucidate the clinical significance.

2. Materials and methods

2.1. Patients and control subjects

Ten symptomatic patients with familial AD (FAD) were recruited from two Taiwanese families. In addition, seven asymptomatic family members who carried this specific gene from the two families were also included for clinical survey and followed up at Chang Gung Memorial Hospital Linkou branch. The enrolled patients underwent a full review of their medical history, detailed physical and neurological examinations, laboratory tests, neuropsychological tests, brain neuroimaging and periodic follow-up interviews. Most of the patients with FAD and the non-symptomatic subjects underwent genetic and neuroimaging studies.

Eighteen age-matched subjects with cognitive decline including ten with mild cognitive impairment (MCI) due to AD and eight with mild to moderate dementia due to AD were individually matched to the cases with familial AD for age, sex, duration of disease and disease severity as assessed by the clinical dementia rating (CDR) scale score. Individual matching was used to avoid selection bias caused by these parameters. All of the subjects with AD were selected according to the New Research criteria [23] including: (i) progressive episodic memory impairment characterized by a loss of free recall, (ii) neuropsychological tests with Alzheimer's Disease Assessment Scale-Cognitive Subscale (ADAS-Cog), and (iii) CDR ≥ 0·5. In addition, 19 HCs with age-matched to symptomatic familial patients were recruited according to the following criteria: (i) Mini-Mental State Examination (MMSE) score ≥ 28/30 and CDR = 0, (ii) no history of neurological or psychiatric disorders, and (iii) no memory complaints or cognitive deficits. All subjects underwent ^{18}F-florbetapir PET tests for amyloid burden.

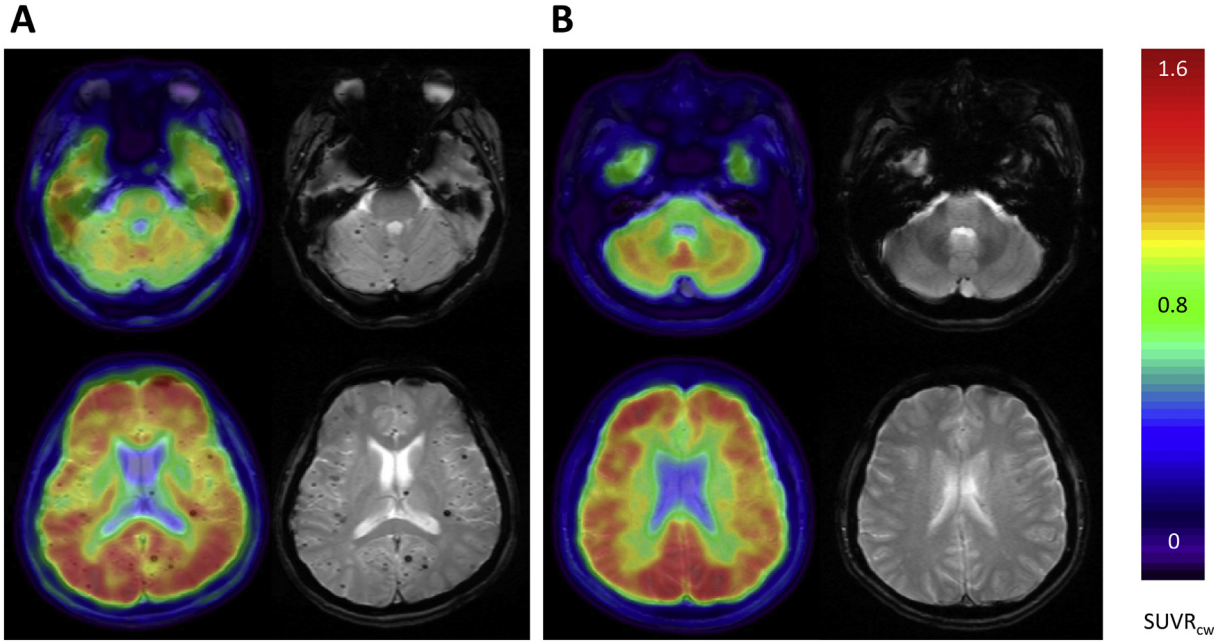

Fig. 2. PET and MRI fusion images of gene-carriers showing cortical and cerebral grey amyloid accumulation in subjects with (A) or without (B) cerebral amyloid angiopathy. (SUVRcw: Standardized uptake value to cerebral white region. the PET images intensity has been normalized to the average counts within the cerebral white matter region).

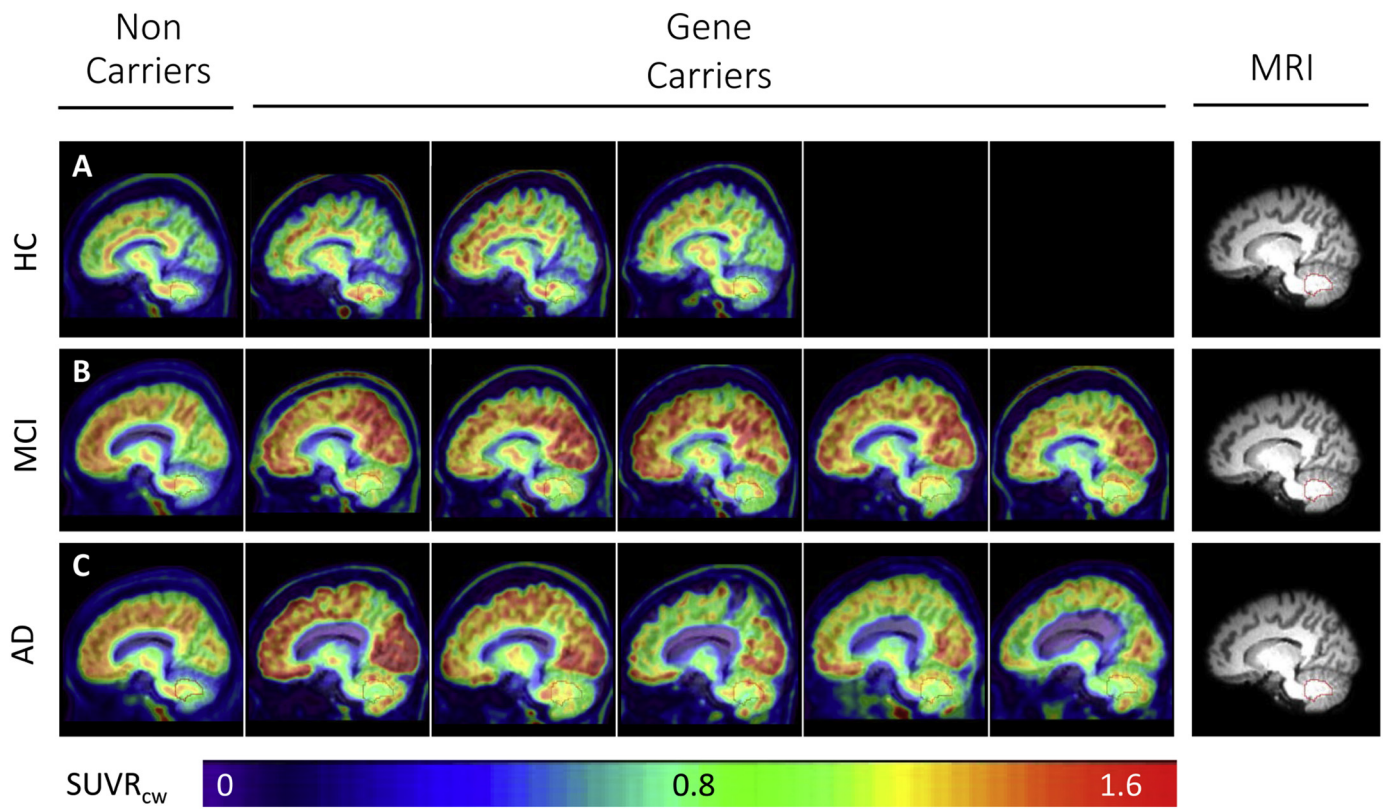

Fig. 3. Sagittal view of PET and MRI fusion images in healthy control (HC), mild cognitive impaired (MCI), and Alzheimer's disease (AD) of non-carriers and gene carriers. The red contour on MRI images indicates the reference region of cerebral white area. (SUVRcw: Standardized uptake value to cerebral white region. the PET images intensity has been normalized to the average counts within the cerebral white matter region).

3. Laboratory examinations

Blood samples were drawn for APoE phenotypes and biochemical studies including complete blood count, liver function, renal function, thyroid function, cortisol, venereal disease research laboratory, vitamin B12, and folic acid. The controls underwent the same procedures as the patients with FAD and AD. Lumbar punctures were not performed due to ethical reasons. The study was approved by the Governmental Department of Health in Taiwan and the Institutional Review Board of Chang Gung Memorial Hospital. All of the participants signed informed consent forms. In addition, the next of kin or guardians of the patients with FAD and AD also gave written informed consent if the patients could not comprehend the study protocol or if they could not sign their names clearly. All of the HCs were either a hospital volunteer or an individual from the surrounding community.

4. Clinical neuropsychological and cognitive assessments

All subjects (FAD, AD and HCs) underwent a clinical and neuropsychological examination. The detailed neuropsychological tests included the MMSE, CDR scale, Wechsler memory scale-revised, visual-association memory test, category verbal fluency test, trail-making A test, and clock-drawing test, all of which were administered to obtain objective evidence of cognitive impairment [24].

5. Mutation analysis of the APP gene

Genomic DNA was extracted from peripheral blood using standard protocols. The exons of PS1, PS2 and APP and exon-intron junctions were polymerase chain reaction (PCR)-amplified as described previously [17,18,25]. PCR fragments then were sequenced in both forward and reverse directions with an ABI 3100 automated DNA sequencer, Applied Biosystems. Mutation analysis involved direct sequencing of PCR-amplified coding exons of the APP gene.

6. Brain MRI procedure

All subjects received an MRI scan with a 3 T MR scanner (Magnetom Trio, a TIM system; Siemens, Erlangen, Germany). The scanning protocol included an axial fluid attenuation inversion recovery (FLAIR) sequence (TR = 9000 ms, TE = 87 ms, TI = 2500 ms, voxel size = 0·9 × 0·7 × 4 mm^3) and a whole brain axial three-dimensional T1-weighted magnetization prepared rapid acquisition gradient echo (MP-RAGE) sequence (TR = 2000 ms, TE = 2·63 ms, TI = 900 ms, flip angle = 9°, voxel size = 1 × 1 × 1 mm^3), which was subsequently reformatted as planes perpendicular to the long axis of the hippocampus in 2-mm slice thicknesses. An additional coronal T2-weighted turbo spin echo sequence (TR = 7400 ms, TE = 95 ms, voxel size = 0·4 × 0·4 × 2 mm^3) was acquired with the identical geometric orientation with the reformatted coronal T1-weighted images.

7. Amyloid PET acquisition

Radiosynthesis and the acquisition of ^{18}F-florbetapir PET images were performed as described previously [26]. In summary, a ^{18}F-florbetapir PET scan was performed using a Biograph mCT PET/CT system (Siemens Medical Solutions, Malvern, PA). A 10-min PET scan was acquired at 50 min post-injection of 375 ± 18 MBq of ^{18}F-florbetapir. The 3-D ordered subsets expectation maximization (OSEM) reconstruction algorithm (four iterations, 24 subsets; Gaussian filter 2 mm, zoom 3) was applied with CT-based attenuation correction and scatter and random corrections, which resulted in reconstructed images with a matrix size of 400 × 400 × 148 and a voxel size of 0·68 × 0·68 × 1·5 mm [27].

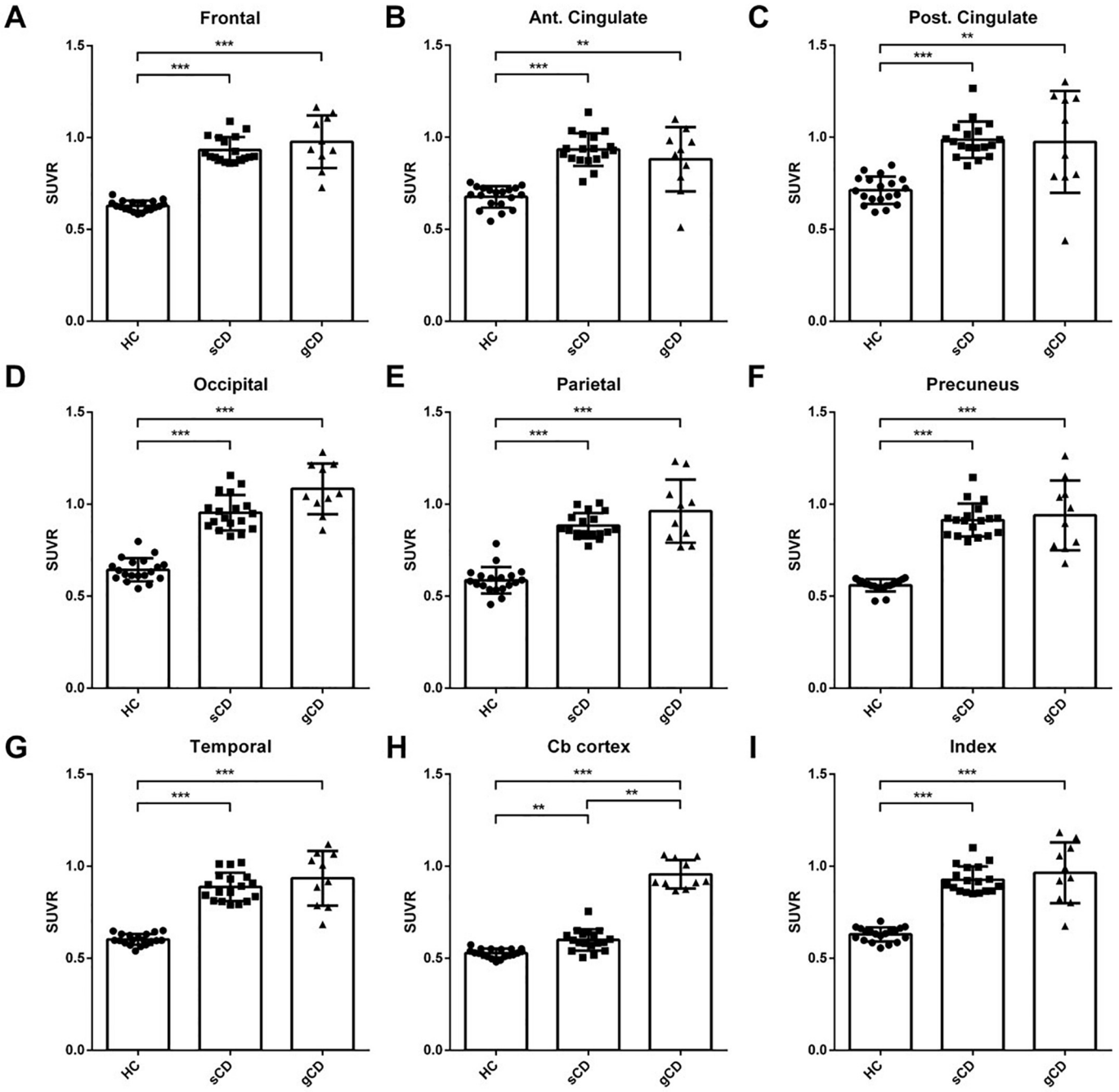

Fig. 4. Group differences in florbetapir SUVR data.
Scatter plots showing all individual florbetapir SUVR data in composite cortical (A-H), and index average (I) for 19 healthy controls (HCs), ten gene-carriers with cognitive decline (gCD), and 18 age-matched subjects presenting with sporadic cognitive decline (sCD).

8. Image analysis

PMOD image analysis software (version 3.3; PMOD Technologies Ltd., Zurich, Switzerland) was used for all image processing and analysis. Each PET image was spatially normalized to the Montreal Neurological Institute (MNI) space using MR-based spatial normalization. Nine volumes of interest (VOIs) including the cerebellum grey, cerebellum white, frontal, anterior cingulate, posterior cingulate, precuneus, parietal, occipital, and temporal areas, were selected based on the modified automated anatomic labelling (AAL) atlas [28]. Voxel-wise SUVR images were calculated using the cerebellum white reference region, and regional SUVRs were measured from the mean SUVR of each VOI. The global index cortical SUVR was calculated from the average SUVR of eight cerebral cortical VOIs for analysis.

8.1. Voxel-wise analysis

The SPM12 software package (Wellcome Department of Cognitive Neurology, Institute of Neurology, London, UK) was used for voxel-wise imaging analysis implemented in Matlab 2010a (MathWorks Inc., Natick, MA). Smoothing was performed using an isotropic Gaussian kernel of 8 mm full-width at half-maximum (FWHM) on the previously spatially-normalized SUVR images of ^{18}F-florbetapir. Two-sample *t*-tests were used to analyse the amyloid SUVR images, and SPM t-maps were examined with a false discovery rate (FDR)-corrected threshold of $P < 0{\cdot}01$ and an extent threshold of 100 voxels for group between the

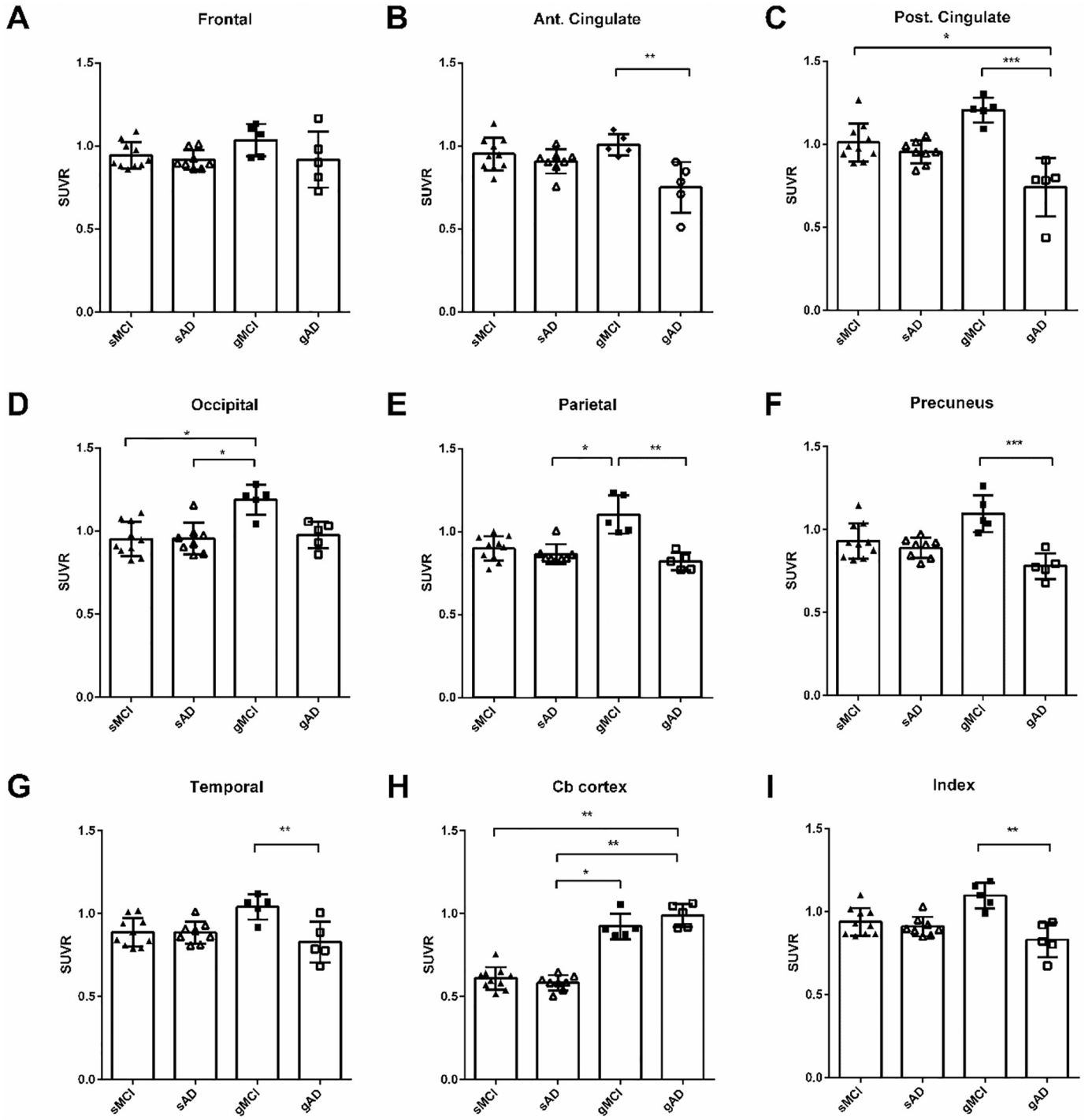

Fig. 5. Scatter plots showing florbetapir SUVR data in cognitive decline subgroups including ten with sporadic mild cognitive impairment (sMCI), eight with sporadic Alzheimer's Disease (sAD), five gene-carriers with mild cognitive impairment (gMCI), and five gene-carriers with Alzheimer's Disease (gAD).

subjects with sporadic cognitive decline (sCD) and gene-carriers with cognitive decline (gCD) and subgroup comparison among those with sporadic MCI (sMCI), sporadic AD (sAD), genetic MCI (gMCI) and genetic AD (gAD).

8.2. Statistical analysis

Data are expressed as means ± SD, or as absolute numbers with proportions for descriptive statistics. The regional SUVRs of the ^{18}F-florbetapir PET images were compared individually region by region using the non-parametric Kruskal-Wallis test with Dunn's multiple comparison post-hoc analysis for group and subgroup comparisons between the 18 subjects with sCD and 10 gene-carriers with cognitive decline (gCD). A p value of 0·05 was taken as the threshold for statistical significance in each test.

9. Results

Fig. 1 shows five and four generations of the two large Taiwanese familial AD pedigrees. The clinical characteristics of the ten symptomatic patients and seven asymptomatic carriers with the specific Taiwanese APP (D678H) mutation are shown in Table 1. Of the ten

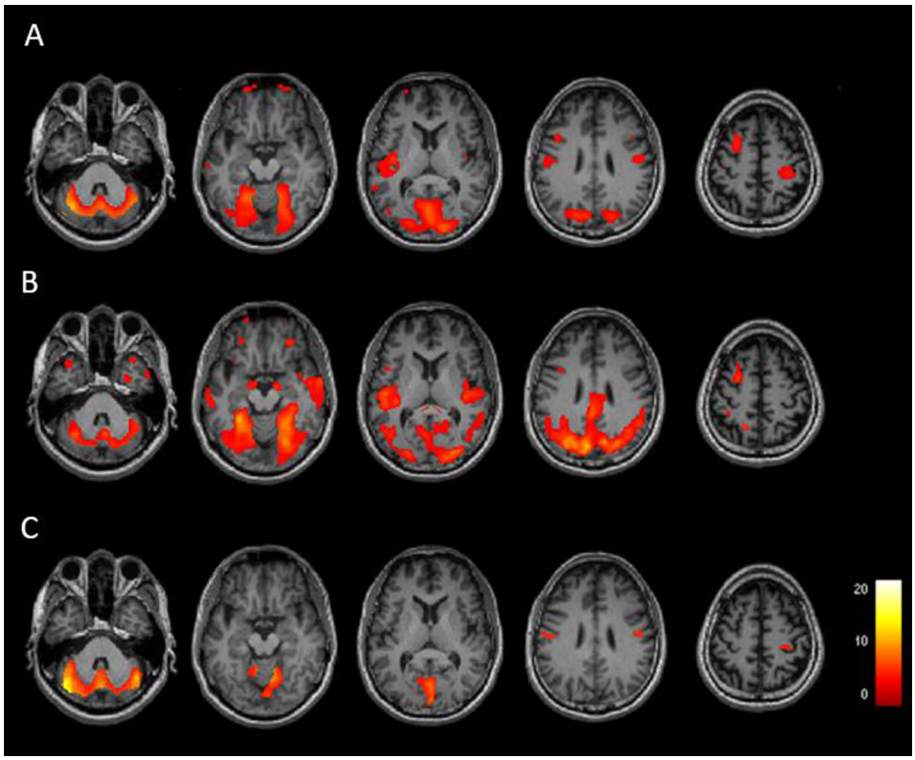

Fig. 6. (A) The results of voxel-based statistical analysis visualizing increased florbetapir uptake in the gene-carriers with cognitive decline (gCD) compared to age-matched subjects presenting with sporadic cognition decline (sCD). Subgroup analysis of the subjects with cognitive decline showing greater amyloid burden in (B) gene-carriers with mild cognitive impairment (gMCI) compared to sporadic subjects (sMCI); and (C) gene-carriers with Alzheimer's Disease (gAD) compared to sporadic subjects (sAD). The colour intensity represents t-statistic values at voxel-level ($p < 0{\cdot}01$, with false discovery rate correction).

symptomatic patients (four men and six women), their current ages ranged from 48 to 72 years, with an age at onset ranging from 46 to 55 years and an education level from 1 to 14 years. The initial symptoms included recent memory impairment in all ten patients, disorientation to time and place in one, delusions/hallucinations in four, and silly laughter in one.

Three patients developed anxiety, irritability and delusions when they saw themselves in a mirror during follow-up. Two patients started talking to themselves and were unable to dress themselves 3–4 years later. No symptoms of slow motion, unsteady gait, masked face, bradykinesia, or rigidity were noted.

The initial MMSE scores ranged from 8 to 28 with initial CDR scores of 0·5 to 2·0. Mutational screening showed that our cohort carried a disease-causing mutation on the APP gene with non-synonymous amino acid substitution (D678H, Asp678His). Table 2 shows the clinical progression and changes in neurocognitive function, brain CT/MRI findings, brain ^{18}F-flobetapir PET findings and treatment. The clinical courses of the symptomatic patients included insidious onset of memory impairment with an initially slow progression. However, within a few years the progression became rapid. The clinical symptoms included recent memory loss in all ten patients with progression to disorientation and delusions/hallucinations in five patients. One patient (patient A-III-3 from family A) had cerebral haemorrhages and a suspected head injury in 2005, and he received surgery for a subdural hematoma with uncal herniation. After the operation, he was in stuporous status and was placed in a nursing home.

Brain CT/MRI scans showed mild cortical atrophy initially to diffuse prominent cortical atrophy in five patients (patient III-3, III-5, and III-6 in family A, and patient II-2 and II-3 in family B), mild cortical atrophy in three patients, and two patients within normal limits (patient A-III-7 and A-IV-2). Multiple cortical microbleeds in brain MRI probably related to cerebral amyloid angiopathy were noted in two patients (patient A-III-3 and patient B-III-5), and ventricular dilatation and diffuse cortical atrophy and post-operative changes were noted in patient A-III-3. In addition, old large haemorrhages in the cerebral hemispheres possibly related to amyloid angiopathy were also noted in patient A-III-3. Brain MRI scans revealed white matter lesions in three patients (patient B-II-2, B-II-3, and B-III-1). The initial brain CT/MRI findings of three asymptomatic family members (subject A-IV-5, A-IV-10, and B-III-6) with the novel mutation were normal. Table 3 shows the demographic data of the 10 familial patients with CD, the 18 patients with sporadic CD and the 19 HCs. The ages of HCs were matched with symptomatic familial cases.

10. Molecular genetic analysis

Sequencing showed a G → C nucleotide substitution in the APP gene that resulted in an aspartate to histidine mutation at the 7th position of Aβ. Mutation analysis of the PCR products from all of the family members showed a positive D678H mutation in all ten symptomatic patients with FAD and the seven asymptomatic family members. This mutation was not found in the other HCs or other sporadic Taiwanese patients with AD. In addition, all of the symptomatic family patients with AD had mutation E3/E3 in the APoE gene except for patient B-III-5 who had E2/E3. The asymptomatic carriers all had the E3/E3 subtype in APoE except for subject B-III-6 (E2/E3) (Table 1).

11. Brain AV-45 PET scan

Brain AV-45 PET images were obtained from the ten symptomatic patients and three asymptomatic carriers. The uptake of ^{18}F-flobetapir was increased in all ten symptomatic patients, particularly in the frontal, temporal, parietal, precuneus and occipital areas. The uptake of SUVR was most prominent in the occipital area in the initial brain ^{18}F-flobetapir PET images. The patients with symptomatic AD had a positive AV-45 PET scan at ages ranging from 47 to 66 years. However, in the three asymptomatic carriers with the D678H APP mutation, the brain ^{18}F-flobetapir PET scans revealed no increase in amyloid uptake at ages ranging from 21 to 45 years. Fig. 2A shows that an increased SUVR of the brain AV-45 PET in the patient B-III-5 who had multiple cortical microbleeds in the brain MRI compatible with cerebral amyloid angiopathy. Fig. 2B shows the other patient A-IV-2 who did not have microbleeds in the initial brain MRI, also had an increased SUVR in the brain AV-45 PET scan.

The amyloid PET and MRI fusion images of the ten symptomatic family gCD including five with MCI and five with AD with the D678H APP mutation and the average images of the 19 HCs (A), ten patients with sporadic MCI due to AD (B), and eight patients with sporadic CD (C) are shown in Fig. 3. The figure reveals a prominent increase in amyloid uptake in the frontal, temporal, parietal, and precuneus areas, and particularly in the occipital area. In addition, when comparing the gCD and subjects with sCD, a greater amyloid burden was noted in the frontal, temporal, occipital, parietal, precuneus, and cerebellar grey matter in five of the familial patients with MCI and five of the familial patients with AD. In this fusion figure with PET/MRI the uptake of SUVR are usually in the cerebellar white matter in the HCs and sMCI.

Fig. 4 shows group differences in the regional SUVRs of 10 gCD versus non-gene-carriers in the 19 HCs, and 18 age-matched subjects with sCD due to AD. The gCD and subjects with sCD had statistically significantly increased SUVRs in the frontal, anterior cingulate, posterior cingulate, occipital, parietal, precuneus, temporal, cerebellar cortex areas and index average ($p < 0{\cdot}01$ and $p < 0{\cdot}001$, respectively) compared with the HCs. In addition, a significantly higher amyloid uptake was also noted in the gCD than the subjects with sCD in the cerebellar grey region ($p < 0{\cdot}01$). In the subgroup analysis among the gMCI, gAD, sMCI, and sAD, the SUVRs were higher in the gMCI than in the gAD in the anterior cingulate, parietal, temporal areas and index average ($p < 0{\cdot}01$), and posterior cingulate and precuneus areas ($p < 0{\cdot}001$), respectively. The SUVRs in the gMCI were also significantly higher in the occipital, parietal, and cerebellar cortex areas ($p < 0{\cdot}05$) compared to the subjects with sAD, and in the occipital area ($p < 0{\cdot}05$) compared to the sMCI group. Amyloid uptake showed a mildly decreasing trend in the gAD group in most brain areas except for cerebellar grey regions compared with the gMCI groups (Fig. 5). Fig. 6 shows the results of voxel-based statistical analysis visualizing increased florbetapir uptake in the gCD compared to the aged-matched subjects with sCD (A). Subgroup analysis of the gMCI showed a greater amyloid burden compared to the sMCI group (B). In addition, the gAD also had a higher amyloid uptake than those with sAD (C). Taken together, these data indicate that the gMCI group had a greater amyloid burden than the sMCI and gAD groups.

12. Discussion

The present study shows the main clinical features of progressive memory impairment followed by rapid progression to severe dementia within 5 to 10 years with an age at onset of around 46–55 years in Taiwanese patients with the novel APP (D678H) mutation. In addition, cerebral amyloid angiopathy with microhemorrhages were noted in two of our symptomatic patients (patient A-III-3 and B-III-5). This mutation is rare and has previously only been reported in two single case reports with no details on family history or follow-up [17,18]. One patient had progressive dementia and the other had cerebral microvasculopathy. Our findings from the two large families may therefore provide detailed and new information on both dementia and amyloid microangiopathy for this specific Taiwan mutation. Other APP mutations have been reported to cause cerebral microangiopathy [9–14], as seen in two of our patients with the specific Taiwan mutation and also in the previous case report [17]. Our findings should also raise awareness of cerebral haemorrhages, particularly during treatment with either active vaccinations or monoclonal antibodies such as Aducanumab which can potentially reduce Aβ plaques in patients with AD [29].

Why the novel Taiwan APP mutation showed such an effect in the family with AD is unclear. The mechanisms remain to be elucidated, however the Aβ N-terminal region may potentially modulate APP processing and Aβ aggregation, particularly altering Aβ at its earliest stages of monomer folding and oligomerization [30,31]. Cellular and biochemical analyses have revealed that this mutation can increase Aβ production, Aβ 42/40 ratio and prolong the Aβ 42 oligomer state [17,32]. In addition, the Aβ D7H mutation has been shown to have an additional metal ion-coordinating residue-histidine, and this has been speculated to promote susceptibility of Aβ to ions such as Zn^{+2} and Cu^{+2} [17]. A previous study also indicated that a high concentration of Zn^{+2} and Cu^{+2} in glutamatergic synapse may promote Aβ aggregation and toxicity [33].

In our brain MRI studies, the changes in the familial patients with AD were very similar to those of the patients with sporadic AD, including atrophy of the hippocampus in the early stage and then diffuse cortical atrophy in the late stage except for patient A-III-7 and A-IV-5 who still had a normal MRI scan. These findings may indicate that amyloid deposition develops much earlier than structural changes in brain MRI. Amyloid microangiopathy was also noted in patient A-III-4 who had ventricular dilatation and changes after surgery for subdural hematoma and amyloid microangiopathy with old haemorrhages in bilateral hemispheres. Patient B-III-3 also had cerebral amyloid angiopathy. In the brain ^{18}F-AV-45 PET study, the most striking finding was increased amyloid uptake in the occipital area and cerebellar cortical area compared to the patients with sAD and the HCs. A visual variant of AD with Aβ burden in posterior cortical atrophy has been reported [34]. Despite a high level of amyloid disposition in the occipital and cerebellar cortex areas in our patients, visual symptoms or cerebellar dysfunction were not found. Several studies have also shown that amyloid burden is not related to clinical symptomatology [35]. Previous studies have reported that amyloid angiopathy is not uniformly distributed in the brain but is rather more likely to occur with an occipital distribution [36,37]. Our family members also had a tendency to develop amyloid angiopathy, and brain AV-45 PET showed a higher amyloid accumulation in the occipital lobe.

To better understand the amyloid deposition pattern, we classified the genetically-positive family member and patients with sporadic AD into four groups: gAD, gMCI, sAD and sMCI. We found that the gMCI group had the highest SUVR of AV-45 in the occipital area compared to the sAD and sMCI groups. In addition, compared to the gAD group, the SUVRs in the gMCI group were significantly higher in the anterior cingulate, posterior cingulate, parietal, precuneus, temporal and global index areas. This may indicate that amyloid uptake is decreased in the later stage. The mechanism remain unclear but is probably related to cortical atrophy as it can lead to brain tissue loss. Another interesting finding is that amyloid could also be deposited much higher in the cerebellar cortical area compared to the patients with sAD and HCs. Occipital and cerebellum amyloid burden may represent a late stage of disease or a more advanced stage of disease. Taken together, these findings imply that the novel Taiwan APP gene may add a potent amyloid pathology. Possible explanations for these peculiar findings include: 1) the novel Taiwan gene has a specific amyloid deposition pattern, 2) the novel mutation induces an amyloid burden in the cerebellar cortex such as in the later stage of patients with sAD, and 3) a possible association with cortical atrophy and ventricular dilatation. 4) interaction between Tau and the amyloid proteins in different stages of FAD.

Further studies of patients with the Taiwan APP gene and Tau PET imaging studies may provide new information and even possible treatment strategies for these patients.

13. Conclusion

Our data indicate that the novel Taiwan APP (D678H) mutation may result in a more potent amyloid burden than in the patients with sporadic AD and HCs. The high amyloid uptake in the occipital area is characteristic of the specific Taiwan APP gene.

Acknowledgements

We would like to express our thanks to Yu-Chen Hsieh for coordinating the study and technical assistance. We thank Avid

Radiopharmaceuticals Inc. (Philadelphia, PA, USA) for providing the precursor for the preparation of ^{18}F-florbetapir. We also thank Chia-Ju Hsieh and Mei-Ping Kung for their initial help for the brain ^{18F}AV-45 PET study.

Conflict of interest

All of the authors have no conflicts of interest

Author contribution

Providing information: CY Huang, WC Hsu, YC Weng, TY Chang, CH Liu, KL Huang, CC Huang.

Conception & design of the study: CC Huang, IT Hsiao, KJ Lin, TC Yen.

Acquisition of data: CY Huang, HC Fung, CC Huang

Table and figures: CY Huang, IT Hsiao, KJ Lin

Analysis and/or interpretation of data: IT Hsiao, CY Huang, CC Huang.

Drafting of the manuscript: CY Huang, CC Huang

Reviewing the manuscript critically: IT Hsiao, KJ Lin, TC Yen, CC Huang.

Reviewing important intellectual content: CC Huang

Approval of the version of manuscript: CC Huang, KJ Lin, TC Yen

Approval of the final version of the paper: All authors

Funding

The study was supported by grants from Ministry of Science and Technology (grant NSC-98-2314-B-182-034-MY2, NSC 98–2314-B-182-056, NSC 100–2314-B-182-003, and NSC-100-2314-B-182-038, MOST 105–2314-B-182-005, MOST 106-2314-B-182-036, MOST 106-2314-B-182A-171) and Chang Gung Memorial Hospital (grant, CMRPG3C0611, and CMRPG3C0612, and CMRPG3E1001, CMRPG3E2191).

References

[1] J.A. Hardy, D.J. Selkoe, The amyloid hypothesis of Alzheimer's disease: progress and problems on the road to therapeutics, Science 297 (2002) 353–356.
[2] R.N. Rosenberg, The molecular and genetic basis of AD: the end of the beginning: the 2000 Wartenberg lecture, Neurology 54 (2000) 2045–2054.
[3] R.E. Tanzi, A genetic dichotomy model for the inheritance of Alzheimer's disease and common age-related disorders, J. Clin. Invest. 104 (1999) 1175–1179.
[4] M. Mullan, F. Crawford, K. Axelman, H. Houlden, L. Lilius, B. Winblad, L. Lannfelt, A pathogenic mutation for probable Alzheimer's disease in APP gene at the N-terminus of beta amyloid, Nat. Genet. 1 (1992) 345–347.
[5] P.H. St George-Hyslop, R.E. Tanzi, P.J. Polinski, J.L. Haines, L. Nee, P.C. Watkins, L. et, The genetic defect causing familial Alzheimer's disease maps on chromosome 21, Science 235 (1987) 885–890.
[6] M.K. Lee, D.R. Borchelt, G. Kim, Thinakaran Gopal, H.H. Slunt, Ratovitski Tamara, et al., Hyperaccumulation of FAD-linked presenilin 1 variants in vivo, Nat. Med. 3 (1997) 756–759.
[7] R. Sherrington, E.I. Rogaev, Y. Liang, E.A. Rogaeva, G. Levesque, M. Ikeda, et al., Cloning of a gene bearing missense mutation in early onset familial Alzheimer's disease, Nature 375 (1995) 754–760.
[8] A. Goate, M.C. Chartier-Harlin, M. Mullan, J. Brown, F. Crawford, L. Fidani, et al., Segregation of a missense mutation in the amyloid precursor protein gene with familial Alzheimer's disease, Nature 349 (1991) 704–706.
[9] J. Haan, J.A. Hardy, R.A. Roos, Hereditary cerebral hemorrhage with amyloidosis-Dutch type: its importance for Alzheimer research, Trends Neurosci. 14 (1991) 231–234.
[10] L. Zhou, N. Brouwers, I. Benilova, A. Vandersteen, M. Mercken, K. Van Laere, et al., Amyloid precursor protein mutation E682K at the alternative β-secretase cleavage β'-site increases Aβ generation, EMBO Mol. Med. 3 (2011) 291–302.
[11] D.A. Carter, E. Desmarais, M. Bellis, D. Campion, F. Clerget-Darpoux, A. Brice, et al., More missense in amyloid gene, Nat. Genet. 2 (1992) 255–256.
[12] J. Armstrong, M. Boada, M.J. Rey, N. Vidal, I. Ferrer, Familial Alzheimer disease associated with A713T mutation in APP, Neurosci. Lett. 11 (2004) 241–243.
[13] L. Hendriks, C.M. van Duign, P. Cras, M. Cruts, W. Van Hul, F. van Harskamp, Presenile dementia and cerebral hemorrhage linked to a mutation at codon 692 of the beta-amyloid precursor protein gene, Nat. Genet. 1 (1992) 218–221.
[14] T.J. Grabowski, H.S. Cho, J.P. Vonsattel, G.W. Rebeck, S.M. Greenberg, Novel amyloid precursor protein mutation in an Iowa family with dementia and severe cerebral amyloid angiopathy, Ann. Neurol. 49 (2001) 697–705.
[15] G. Di Fede, M. Catania, M. Morbin, G. Rossi, S. Suardi, G. Mazzoleni, et al., A recessive mutation in the APP gene with dominant-negative effect on amyloidogenesis, Science 323 (2009) 1473–1477.
[16] K. Sleegers, N. Brouwers, I. Gijselinck, J. Theuns, D. Goossens, J. Wauters, et al., APP duplication is sufficient to cause early onset Alzheimer's dementia with cerebral amyloid angiopathy, Brain 129 (2006) 2977–2983.
[17] W.T. Chen, C.J. Hong, Y.T. Lin, W.H. Chang, H.T. Huang, J.Y. Liao, et al., Amyloid-beta (Aβ) D7H mutation increases oligomeric Aβ42 and alters properties of Aβ-Zinc/copper assemblies, PLoS One 7 (2012) e34666.
[18] M.Y. Lan, J.S. Liu, Y.S. Wu, C.H. Peng, Y.Y. Chang, A novel APP mutation (D678H) in a Taiwanese patient exhibiting dementia and cerebral microvasculopathy, J. Clin. Neurosci. 21 (2013) 513–515.
[19] Jack CR Jr, Lowe VJ, Weigand SD, Wiste HJ, Senjem ML, Knopman DS, et al. Serial PiB and MRI in normal, mild cognitive impairment and Alzheimer's disease: implications for sequence of pathological events in Alzheimer's disease. 2009; Brain 132: 1355–65.
[20] C.R. Jack, D.S. Knopman, W.J. Jagust, L.M. Shaw, P.S. Aisen, M.W. Weiner, et al., Hypothetical model of dynamic biomarkers of the Alzheimer's pathological cascade, Lancet Neurol. 9 (2010) 119–128.
[21] C.M. Clark, J.A. Schneider, B.J. Bedell, T.G. Beach, W.B. Bilker, M.A. Mintun, et al., Use of florbetapir PET for imaging beta-amyloid pathology, JAMA 305 (2011) 275–283.
[22] K.L. Huang, K.J. Lin, I.T. Hsiao, H.C. Kuo, W.C. Hsu, W.L. Chuang, et al., Regional amyloid deposition in amnestic mild cognitive impairment and Alzheimer's disease evaluated by ^{18}F-AV-45 positron emission tomography in Chinese population, PLoS One 8 (2013) e58974.
[23] Mckhann GM, Knopman DS, Chertkow H, Hyman BT, Jack CR Jr, Kawas CH, et al. The diagnosis of dementia due to Alzheimer's disease: Recommendations from the National Institute on aging and the Alzheimer's association workgroup. Alzheimers Dement. 2011; 7: 263–9.
[24] P.N. Wang, C.J. Hong, K.N. Lin, H.C. Liu, W.T. Chen, APOE episilon 4 increase the risk of progression from amnestic mild cognitive impairment to Alzheimer's disease among ethnic Chinese in Taiwan, J. Neurol. Neurosurg. Psychiatry 82 (2011) 165–169.
[25] N.S. Ryan, J.M. Nicholas, P.S. Weston, Y. Liang, T. Lashley, R. Guerreiro, et al., Clinical phenotype and genetic associations in autosomal dominant familial Alzheimer's disease: a case series, Lancet Neurol. 15 (2016) 1326–1335.
[26] C.H. Yao, K.J. Lin, C.C. Weng, I.T. Hsiao, Y.S. Ting, T.C. Yen, et al., GMP-compliant automated synthesis of [(18)F]AV-45 (Florbetapir F 18) for imaging beta-amyloid plaques in human brain, Appl. Radiat. Isot. 68 (2010) 2293–2297.
[27] K.J. Lin, W.C. Hsu, I.T. Hsiao, S.P. Wey, L.W. Jin, D. Skovronsky, et al., Whole-body biodistribution and brain PET imaging with [18F]AV-45, a novel amyloid imaging agent–a pilot study, Nucl. Med. Biol. 37 (2010) 497–508.
[28] K.Y. Wu, C.Y. Liu, C.S. Chen, C.H. Chen, I.T. Hsiao, C.J. Hsieh, et al., Beta-amyloid deposition and cognitive function in patients with major depressive disorder with different subtypes of mild cognitive impairment: F-florbetapir (AV-45/Amyvid) PET study, Eur. J. Nucl. Med. Mol. Imaging 43 (2016) 1067–1076.
[29] J. Sevigny, P. Chiao, T. Bussière, P.H. Weinreb, L. Willians, M. Maier, et al., The antibody aducanumab reduces Aβ plaques in Alzheimer's disease, Nature 537 (2016) 50–56.
[30] Y. Wakutani, K. Watanabe, Y. Adachi, K. Wada-Isoe, K. Urakami, H. Ninomiya, et al., Novel amyloid precursor protein gene missense mutation (D678N) in probable familial Alzheimer's disease, J. Neurol. Neurosurg. Psychiatry 75 (2004) 1039–1042.
[31] K. Ono, M.M. Condron, D.B. Teplow, Effects of the English (H6R) and Tottori (D7N) familial Alzheimer disease mutations on amyloid beta-protein assembly and toxicity, J. Biol. Chem. 285 (2010) 23186–23197.
[32] Y.C. Lin, J.Y. Wang, K.C. Wang, J.Y. Liao, I.H. Cheng, Differential regulation of amyloid precursor protein sorting with pathological mutations results in a distinct effect on amyloid-β production, J. Neurochem. 131 (2014) 407–412.
[33] J.A. Duce, A.I. Bush, Biological metals and Alzheimer's disease: Implications for therapeutics and diagnostics, Prog Neuobiol 92 (2010) 1–18.
[34] D.F. Benson, R.J. Davis, B.D. Snyder, Posterior cortical atrophy, Arch Neural 45 (1988) 789–793.
[35] G.D. Rabinovici, A.J. Furst, A. Alkalay, C.A. Racine, J.P. O'Neil, M. Janabi, et al., Increased metabolic vulnerability in early-onset Alzheimer's disease is not related to amyloid burden, Brain 133 (2010) 512–528.
[36] K.A. Johnson, M. Gregas, J.A. Becker, Kinnecom Catherine, D.H. Salat, E.K. Moran, et al., Imaging of amyloid burden and distribution in cerebral amyloid angiopathy, Ann. Neurol. 62 (2007) 229–234.
[37] J. Rosand, A. Muzikansky, A. Kumar, J.J. Wisco, E.E. Smith, R.A. Betensky, et al., Spatial clustering of hemorrhages in probable cerebral amyloid angiopathy, Ann. Neurol. 58 (2005) 459–462.